

# Astrometry of H<sub>2</sub>O Masers in Nearby Star-Forming Regions with VERA — IV. L1448C

Tomoya HIROTA,<sup>1,2</sup> Mareki HONMA,<sup>1,2</sup> Hiroshi IMAI,<sup>3</sup> Kazuyoshi SUNADA,<sup>2,4</sup>  
YuJi UENO,<sup>4</sup> Hideyuki KOBAYASHI,<sup>1,5</sup> Noriyuki KAWAGUCHI,<sup>2,4</sup>

<sup>1</sup>*Mizusawa VLBI Observatory, National Astronomical Observatory of Japan,  
2-21-1 Osawa, Mitaka, Tokyo 181-8588*

<sup>2</sup>*Department of Astronomical Sciences, Graduate University for Advanced Studies,  
2-21-1 Osawa, Mitaka, Tokyo 181-8588*

<sup>3</sup>*Graduate School of Science and Engineering, Kagoshima University,  
1-21-35 Korimoto, Kagoshima, Kagoshima 890-0065*

<sup>4</sup>*Mizusawa VLBI Observatory, National Astronomical Observatory of Japan,  
2-12 Hoshi-ga-oka, Mizusawa-ku, Oshu-shi, Iwate 023-0861*

<sup>5</sup>*Department of Astronomy, Graduate School of Science, The University of Tokyo,  
7-3-1 Hongo, Bunkyo-ku, Tokyo 113-0033  
tomoya.hirota@nao.ac.jp*

(Received 2010 June 1; accepted 2010 0)

## Abstract

We have carried out multi-epoch VLBI observations with VERA (VLBI Exploration of Radio Astrometry) of the 22 GHz H<sub>2</sub>O masers associated with a Class 0 protostar L1448C in the Perseus molecular cloud. The maser features trace the base of collimated bipolar jet driven by one of the infrared counter parts of L1448C named as L1448C(N) or L1448-mm A. We detected possible evidences for apparent acceleration and precession of the jet according to the three-dimensional velocity structure. Based on the phase-referencing VLBI astrometry, we have successfully detected an annual parallax of the H<sub>2</sub>O maser in L1448C to be  $4.31 \pm 0.33$  milliarcseconds (mas) which corresponds to a distance of  $232 \pm 18$  pc from the Sun. The present result is in good agreement with that of another H<sub>2</sub>O maser source NGC 1333 SVS13A in the Perseus molecular cloud, 235 pc. It is also consistent with the photometric distance, 220 pc. Thus, the distance to the western part of the Perseus molecular cloud complex would be constrained to be about 235 pc rather than the larger value, 300 pc, previously reported.

**Key words:** Astrometry: — ISM: individual (L1448C) — ISM: jets and outflows — masers (H<sub>2</sub>O) — stars: individual (L1448C)

## 1. Introduction

In order to understand formation processes of stars, it is necessary to obtain accurate physical and dynamical properties of newly born young stellar objects (YSOs) such as size, mass, and luminosity. For this purpose, an accurate distance to a YSO in a star-forming region is the most fundamental parameter for quantitative discussion. In the last decade, great efforts have been made to establish the highest accuracy astrometric observations with the very long baseline interferometry (VLBI). This, VLBI astrometry, enables to measure annual parallaxes for bright radio sources, i.e. maser sources and non-thermal radio sources, associated with YSOs at a typical accuracy of sub-milliarcseconds (mas). It can achieve much better accuracy by 2-3 orders of magnitude than that of the optical astrometry satellite Hipparcos (Perryman et al. 1997). As a result, the distances to several well studied star-forming regions such as Taurus (Loinard et al. 2005; Loinard et al. 2007; Torres et al. 2007; Torres et al. 2009), Ophiuchus (Imai et al. 2007; Loinard et al. 2008), Orion (Hirota et al. 2007; Sandstrom et al. 2007; Menten et al. 2007; Kim et al. 2008), Perseus (Hirota et al. 2008a), and Cepheus (Hirota et al. 2008b; Moscadelli et al. 2009) regions were refined with better than a few percent uncertainties.

Among them, we have been carrying out a VLBI astrometry project "Measurements of annual parallaxes of nearby molecular clouds" with VERA (VLBI Exploration of Radio Astrometry). VERA is a Japanese VLBI network operated by National Astronomical Observatory of Japan (NAOJ) and Kagoshima University. VERA is designed to dedicate for astrometric observations aimed at revealing three-dimensional structure of the Galaxy (e.g. Honma et al. 2007). Our project mainly focuses on the accurate distance measurements of star-forming regions within 1 kpc from the Sun (Dame et al. 1987; Evans et al. 2003). Part of the results have been reported in a series of papers (Hirota et al. 2007; Imai et al. 2007; Hirota et al. 2008a; Hirota et al. 2008b; Kim et al. 2008).

Here we present a new result of our VLBI astrometry of the H<sub>2</sub>O masers associated with L1448C (or L1448-mm) in an optical dark cloud Lynds 1448 (Lynds 1962). L1448 is located at 1 degree southwest of another star-forming region NGC 1333 (Hirota et al. 2008a) in the Perseus molecular cloud. L1448C was first detected at the millimeter (Bachiller et al. 1991) and centimeter (Curiel et al. 1990) wavelengths, and was later classified as a deeply embedded Class 0 protostar based on its spectral energy distribution (SED) from the infrared to millimeter wavelengths (Barsony et al. 1998). Recent observations with the Spitzer Space Telescope revealed that L1448C consists of two infrared counterpart named as L1448C(N) and L1448C(S) (Jørgensen et al. 2006) or L1448-mm A and B (Tobin et al. 2007) which are separated by 8'' as shown in Figure 1. These infrared sources have been observed more recently with the higher resolution interferometers at the centimeter to submillimeter wavelengths (Reipurth et al. 2002; Hirano et al. 2010). L1448C is known to drive large-scale extremely high-velocity molecular outflow traced by the millimeter rotational lines of the CO and SiO molecules (Bachiller et

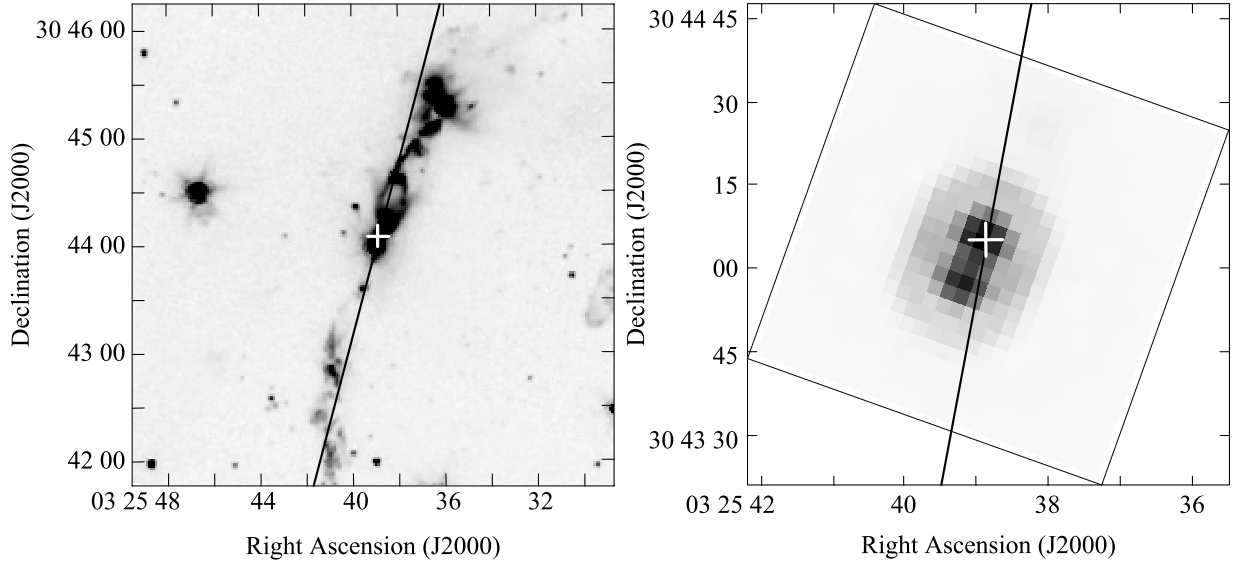


**Fig. 1.** Spitzer IRAC channel 2 image (left) and MIPS channel 1 image (right) of L1448C taken from the Spitzer Legacy Program "From Molecular Cores to Planet Forming Disks" (Evans et al. 2003). A white cross represents the reference position adopted in the present study. A black solid line represents the average position angle of the  $\text{H}_2\text{O}$  maser features in L1448C.

al. 1990; Bachiller et al. 1995; Girart & Acord 2001; Hirano et al. 2010) and the vibrationally excited  $\text{H}_2$  line in the near infrared wavelength (Bally et al. 1993). Thus, L1448C is one of the ideal laboratories to study in detail about the mass-loss processes through the collimated jet and molecular outflow, as well as the nature of the protostar in very young evolutionary phase, and hence, the accurate distance measurement is essential for this purpose. The  $\text{H}_2\text{O}$  masers were detected with single-dish telescopes (Claussen et al. 1996) and the Very Large Array (VLA) (Chernin 1995). However, this is the first time to observe the  $\text{H}_2\text{O}$  masers associated with L1448C with VLBI. The highest resolution observations with VERA yield the proper motions of the masers along with the annual parallax of L1448C.

## 2. Observations and Data Analyses

Observations of the  $\text{H}_2\text{O}$  maser line ( $6_{16}-5_{23}$ , 22235.080 MHz) associated with L1448C were conducted with VERA from November 2007 to February 2009. All 4 stations of VERA (see Fig.1 of Petrov et al. 2007) took part in all observing sessions, providing a maximum baseline length of 2270 km.

Observations were made in the dual beam mode; the  $\text{H}_2\text{O}$  masers associated with L1448C and an extragalactic radio source J0319+3101 (Petrov et al. 2006), with a separation angle of  $1.37^\circ$ , were observed simultaneously. The instrumental phase difference between the two beams was measured continuously during the observations by injecting artificial noise sources into both beams at each station (Honma et al. 2003; Honma et al. 2008a).

Left-handed circular polarization was received and sampled with 2-bit quantization and filtered using the VERA digital filter unit (Iguchi et al. 2005). The data were recorded onto magnetic tapes at a rate of 1024 Mbps, providing a total bandwidth of 256 MHz in which one IF channel and the rest of 15 IF channels with a 16 MHz bandwidth each were assigned to L1448C and J0319+3101, respectively. A bright extragalactic radio source, 3C84, was observed every 80 minutes as a delay and bandpass calibrator. Amplitude calibrations were done through the chopper-wheel method (Ulich & Haas 1976). Correlation processing was carried out on the Mitaka FX correlator (Chikada et al. 1991) located at the NAOJ Mitaka campus. For the H<sub>2</sub>O maser line, the spectral resolution was set to be 15.625 kHz, corresponding to the velocity resolution of 0.21 km s<sup>-1</sup>.

Data reduction was performed using the National Radio Astronomy Observatory (NRAO) Astronomical Image Processing System (AIPS). We first applied the results of the dual-beam phase calibration as mentioned above and the correction for the approximate delay model adopted in the correlation processing. Details in this procedure are described in previous papers (Honma et al. 2003; Honma et al. 2007; Honma et al. 2008a; Honma et al. 2008b). The reference position of L1448C was set to be the geometric center of two maser features as discussed later, RA(J2000)=03h25m38.87840s and Dec(J2000)=+30°44′05″.2516, in the recalculation of the delay tracking model. Next, we calibrated the instrumental delays and phase offsets among all of the IF channels by the AIPS task FRING on 3C84. Finally, we calibrated residual phases by the AIPS task FRING on J0319+3101. The solutions were applied to the target source L1448C. The reference source J0319+3101 has a flux density of only 30 mJy beam<sup>-1</sup> at 22 GHz and hence, it was only marginally detected with the signal-to-noise ratio of about 5 during most of the observing sessions. Therefore, we also calibrated the residual phases by the AIPS task FRING on the intense spectral feature of the H<sub>2</sub>O maser in L1448C instead of J0319+3101. In this case, the solutions were also applied to J0319+3101. These two results will be compared in the later section.

Synthesis imaging and deconvolution (CLEAN) were performed using the AIPS task IMAGR. The uniform weighted synthesized beam size (FWMH) was typically 1.2 mas×0.8 mas with a position angle of -50 degrees. The peak positions and flux densities of masers were derived by fitting elliptical Gaussian brightness distributions to each spectral channel map using the AIPS task SAD. The formal uncertainties in the maser positions given by SAD were better than 0.1 mas. The rms noise levels in the self-calibrated images are 1-2 mJy beam<sup>-1</sup> for J0319+3101 and 50-150 mJy beam<sup>-1</sup> for the channel maps of the L1448C masers with the net integration time of about 3 hours.

### 3. Results

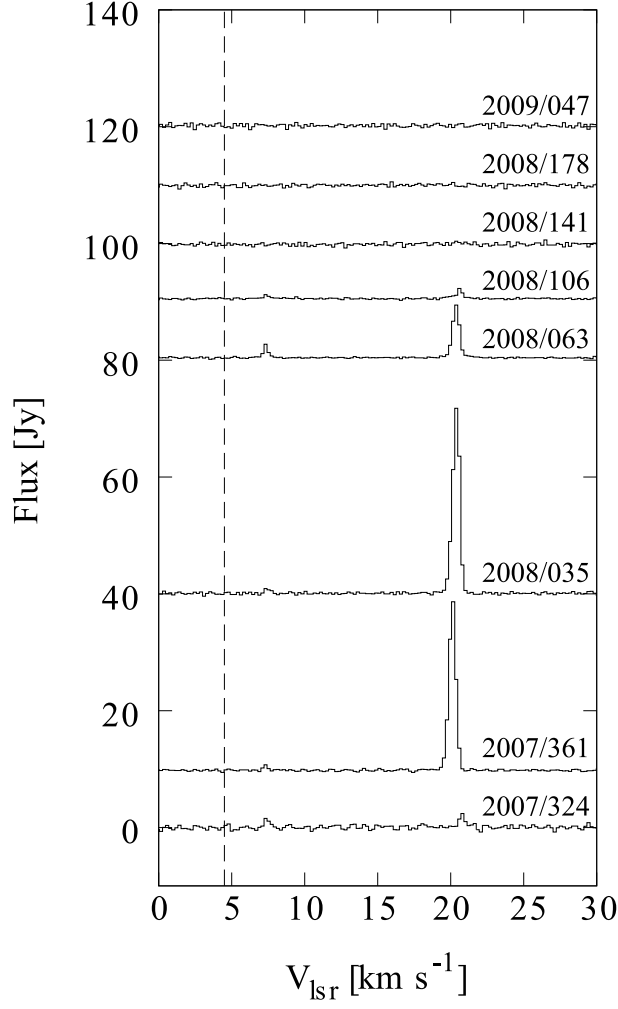
#### 3.1. Structure of the $H_2O$ maser features

Figure 2 shows the spectra of the  $H_2O$  masers associated with L1448C. We detected the masers at five observing sessions, 2007/324, 2007/361, 2008/035, 2008/063, and 2008/106 (denoted by year/day of the year). For later sessions, 2008/141, 2008/178, and 2009/047, we could not detect the masers due to the time variation which is characteristic for the  $H_2O$  masers associated with low-mass protostars (Claussen et al. 1996). The most intense feature was always at the local standard of rest (LSR) velocity of about  $20 \text{ km s}^{-1}$ . The second weak feature was detected at the LSR velocity of  $7 \text{ km s}^{-1}$  from 2007/324 to 2008/106, although they are marginally seen in Figure 2. Both features are red-shifted with respect to the systemic velocity of the molecular cloud L1448,  $4.5 \text{ km s}^{-1}$  (Bachiller et al. 1990). The velocities of the masers are within that of the molecular outflow ranging up to  $\pm 70 \text{ km s}^{-1}$  with respect to the systemic velocity (Bachiller et al. 1990; Bachiller et al. 1995). These two features had been identified by Chernin (1995) whereas we could not detect other velocity components detected by Chernin (1995) and Claussen et al. (1996). We also detected another faint maser feature in 2009/047 at the LSR velocity of  $-24 \text{ km s}^{-1}$ . Because this feature could not be detected in the VLBI imaging, we will exclude this feature in the following discussion.

The distribution of the maser spots are shown in Figure 3. Hereafter we define a “spot” as emission occurring in a single velocity channel and a “feature” as a group of spots. We define two features; one is located at northwest of the reference position while another at southeast.

In order to obtain absolute positions of the maser spots, we at first made synthesis imaging for each epoch by employing the result of the phase-calibration on the reference maser spot at the LSR velocity of  $20.6 \text{ km s}^{-1}$ . This is because we could obtain higher sensitivity images compared with those obtained by phase-referencing to J0319+3101 or other maser spots at different velocities. In this case, positions of the maser spots are measured with respect to the reference spot. Next, we transferred the phase-calibration results to the J0319+3101 data. The absolute position of J0319+3101 has been determined with an uncertainty of 1.63 and 1.68 mas in right ascension and declination, respectively (Petrov et al. 2006), so that we could convert the position offsets of the maser spots with respect to J0319+3101 into absolute positions.

As a result, we can easily locate the absolute position of the maser source to be one of the Spitzer sources, L1448C(N)/L1448-mm A (Jørgensen et al. 2006; Tobin et al. 2007) as shown in Figure 1. The position also agrees well with that of the radio continuum source (Reipurth et al. 2002) and the submillimeter continuum source (Hirano et al. 2010). Note that the positions of the continuum source obtained by the interferometer observations (Reipurth et al. 2002; Hirano et al. 2010) tend to be shifted toward  $0.12\text{--}0.17''$  northwest of our reference position. Although the astrometric accuracies seem to be insufficient with the beam sizes of  $0.3''\text{--}0.7''$  achieved by these observations, the powering source of the masers could be located at



**Fig. 2.** Scalar-averaged cross power spectra of the  $\text{H}_2\text{O}$  maser lines associated with L1448C. A dashed line represents the systemic velocity of  $4.5 \text{ km s}^{-1}$  (Bachiller et al. 1990). The spectra are the averages of those observed at all the VERA stations.

the northwest of the maser images shown in Figure 3.

The spatial distribution of the  $\text{H}_2\text{O}$  masers linearly aligned with a collimated jet-like structure seems to be analogous to the large scale molecular outflow, although the size of the maser structure is much smaller by 3-4 orders of magnitude. The width of the  $\text{H}_2\text{O}$  maser jet is less than 5 mas while its length is 60 mas as can be seen in Figure 3. This scale is significantly smaller than that found by Chernin (1995), 280 mas. The estimated size gives the lower limit for only part of the (red-shifted) jet because we could not detect the blue-shifted  $\text{H}_2\text{O}$  maser jet in the present study. Details of the spatial and velocity structure of the maser features will be discussed in the later section.

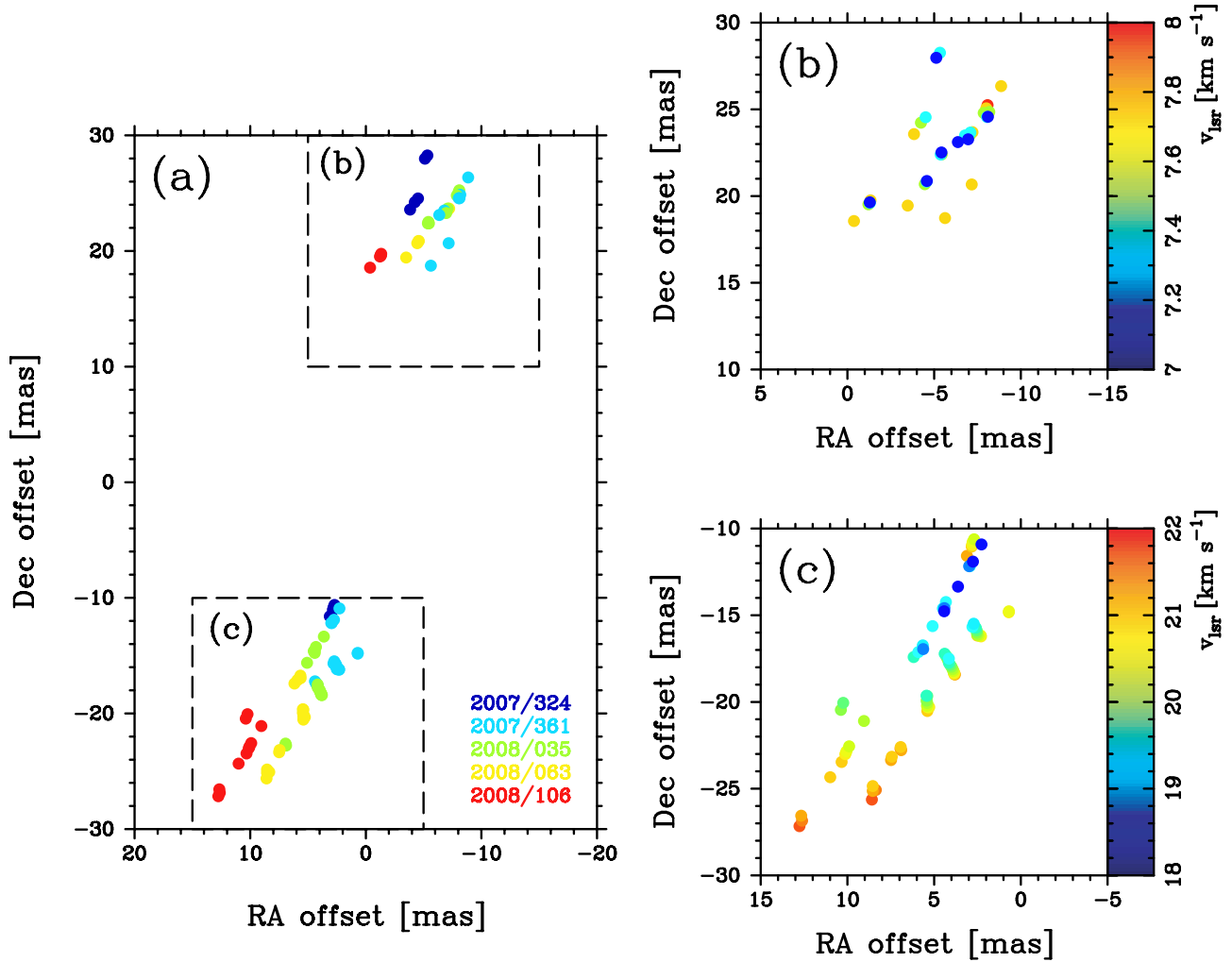


**Fig. 3.** Distribution of  $\text{H}_2\text{O}$  maser spots associated with L1448C. (a) Overall distribution of the maser spots. Each color represents the observed epoch. (b) Close-up of the northern maser feature as indicated by the dashed rectangle in panel (a). Color-coded symbols represent the positions and LSR velocities of the maser spots for all of the observed epochs. (c) Same as (b) but for the southern maser feature. The reference position,  $\alpha(J2000) = 03^{\text{h}}25^{\text{m}}38.87840^{\text{s}}$ ,  $\delta(J2000) = +30^{\circ}44'05''.2516$ , is determined with respect to the position of J0319+3101.

### 3.2. Astrometry of the $\text{H}_2\text{O}$ masers in L1448C

We have successfully determined the absolute positions of the maser spots by referring to the position reference source J0319+3101. In the data analysis, we performed phase-calibration on either the intense maser spot in L1448C or continuum source J0319+3101 as mentioned above. Table 1 compares the results of both methods. Except for the epoch 2007/324 and 2008/106, where L1448C could not be detected by phase-referencing to the J0319+3101, derived position offsets are consistent with each other. The uncertainties of about 0.3 mas (as summarized in the fourth column in Table 1) would be a result of low signal-to-noise ratio of J0319+3101 or structure in the maser spots. The peak fluxes of J0319+3101 obtained by phase-



**Table 1.** Position offsets of the reference maser spots ( $v_{lsr}=20.6 \text{ km s}^{-1}$ ) derived from the phase-referencing methods

	reference: L1448C <sup>a</sup>	reference: J0319 <sup>b</sup>	difference
epoch	$(\alpha, \delta)$	$(\alpha, \delta)$	$(\Delta\alpha, \Delta\delta)$
2007/324	(2.77, -10.80)	—	—
2007/361	(2.35, -16.20)	(2.07, -16.15)	(0.28, -0.05)
2008/035	(3.85, -18.28)	(3.57, -18.42)	(0.28, 0.14)
2008/063	(5.40, -20.35)	(5.26, -20.50)	(0.14, 0.15)
2008/106	(10.07, -22.86)	—	—

*a*: Phase calibrations were done for L1448C and the results were transferred to J0319+3101.

*b*: Phase calibrations were done for J0319+3101 and the results were transferred to L1448C.

Note — The position offsets are measured with respect to the reference position of the masers in unit of milliarcseconds (mas).

referencing to the maser spots of L1448C recover 29% and 52-55% of those of self-calibrated images for 2007/324 and rest of 4 epochs, respectively. On the other hand, phase-referenced image of the maser spots only recover 23-44% of those of self-calibrated image for the epoch 2007/361, 2008/035, and 2008/063. This is due to larger coherence loss in phase calibration on J0319+3101 with the lower signal-to-noise ratio. Thus, we hereafter employ the astrometric results obtained by phase-referencing to the reference maser spot in L1448C.

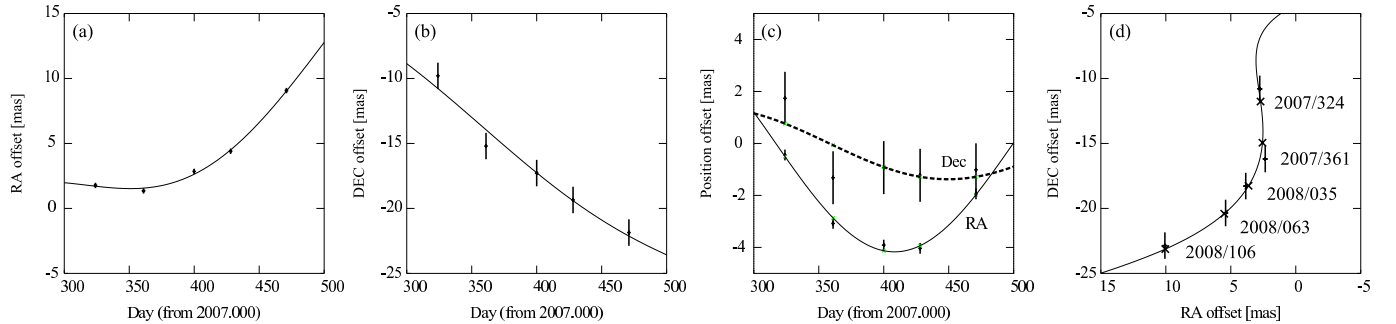


**Fig. 4.** Position measurements of the maser spots at  $v_{lsr} = 20.6 \text{ km s}^{-1}$ . (a) The movement in right ascension as a function of time. (b) The same as (a) but in declination. (c) The same as (a) and (b) but the best fit proper motions are removed. (d) The movement of the maser spots on the sky plane. Solid lines represent the best fit model of the annual parallax. The associated error bars, 0.21 mas and 1.02 mas in right ascension and declination, respectively, are also plotted. Small crosses in panel (c) indicate the expected position for each epoch as labeled in the figure.

Figure 4 shows the position offsets of the masers as a function of observing epoch. The



**Table 2.** Results of the least-squares analysis for the annual parallax and proper motion measurements

Parameter	Best fit value
$\pi$ (mas)	4.31(33)
$D$ (pc)	232(18)
$\mu_\alpha \cos \delta$ (mas yr $^{-1}$ )	21.9(7)
$\mu_\delta$ (mas yr $^{-1}$ )	-23.1(33)
$\mu$ (mas yr $^{-1}$ )	31.8(34)
$v_t$ (km s $^{-1}$ )	35.3(37)
PA (degrees)	137
$\sigma_\alpha$ (mas)	0.19
$\sigma_\delta$ (mas)	0.93

Note — Numbers in parenthesis represent the errors in unit of the last significant digits.  $\sigma_\alpha$  and  $\sigma_\delta$  are the the post-fit residuals.

movement of the masers significantly deviates from a simple linear motion, and it can be fitted as a combination of linear proper motion and the annual parallax by the least-squares analysis. The results of the fitting are summarized in Table 2. Using both the right ascension and declination data, the annual parallax of L1448C is derived to be  $4.31 \pm 0.33$  mas, corresponding to the distance of  $232 \pm 18$  pc from the Sun. The standard deviations of the post-fit residuals are  $\sigma_\alpha = 0.19$  mas and  $\sigma_\delta = 0.93$  mas in right ascension and declination, respectively.

The larger residual in declination is due to position errors in the observations at 2007/361 and possibly 2007/324 as can be seen in Figures 4(b) and (c). These errors are significantly larger than the formal errors in the Gaussian fitting of the maser spots, 0.03-0.1 mas. Therefore, we introduced the error floor of 0.21 mas and 1.02 mas in right ascension and declination, respectively, for all the results of the position measurements to make reduced  $\chi^2$  to be unity in the least-squares analysis. These error floors represent the positional uncertainties in the present astrometric observations. The possible origin of these uncertainties is most likely due to the difference in the optical path lengths between the target and reference sources caused by the atmospheric zenith delay residual and/or a variability of the structure of the maser feature (see detailed discussions in Honma et al. 2007, Hirota et al. 2007, Hirota et al. 2008a, Hirota et al. 2008b).

Based on the simulation by Honma et al. (2008b), positional errors due to the typical zenith delay residual in the VERA observations, 2 cm, can be estimated to be 0.03 mas and 0.01 mas in right ascension and declination, respectively, in the condition close to the present observations (i.e. the separation angle of 1.37 degrees, position angle on the sky from the

target sources to the reference sources of 90 degrees, and the source declination of 15 degrees are employed). Although the assumed value of declination is different from that of L1448C, the estimated position offsets are much smaller than the observed results. Therefore, only the zenith delay residual would not be the cause of the large positional uncertainties unless unexpectedly large zenith delay residuals remain in the data.

The larger positional uncertainties found in the H<sub>2</sub>O masers associated with nearby low-mass YSOs (Hirota et al. 2007; Imai et al. 2007; Hirota et al. 2008a; Hirota et al. 2008b) than in the distant massive YSOs (e.g. Honma et al. 2007) are possibly attributed to the source structure. In fact, such a variation of the internal maser structures have been observed directly by the recent VLBI observations of the H<sub>2</sub>O masers in a nearby low-mass YSO, NGC 1333 IRAS4 (Marvel et al. 2008; Desmurs et al. 2009), with typical timescale of as short as 2-4 weeks. This may strongly affect the results of identifications for H<sub>2</sub>O maser spots between two consecutive epochs separated by only 1 month.

Nevertheless, we can obtain the consistent result,  $\pi=4.30\pm0.37$  mas and  $\sigma_\alpha=0.23$  mas, even if only the right ascension data are used in the least-squares analysis. When we fit the data excluding those of the second epoch 2007/361, the resultant parallax value is consistent within the mutual error ( $4.23\pm0.29$  mas). In this case, the post-fit residuals,  $\sigma_\alpha=0.15$  mas and  $\sigma_\delta=0.39$  mas in right ascension and declination, respectively, are reduced. Unfortunately, the masers associated with L1448C disappeared after the 6-month monitoring observations with VERA, which is also similar to the case for NGC 1333 SVS13A (Hirota et al. 2008a). If the above error sources affect the position measurements as a random noise, the accuracy of the parallax measurement could be improved by increasing the number of observed epochs as well as the detected maser spots. Thus, we need to continue longer monitoring observations of the H<sub>2</sub>O maser sources to improve the accuracy of the annual parallax measurements with VERA.

## 4. Discussions

### 4.1. Collimated H<sub>2</sub>O maser jet from L1448C

Both the spectra and distribution of the maser spots as shown in Figures 2 and 3 imply that the masers trace the base of the protostellar jet driven by the Class 0 source L1448C. In this section, we will discuss about the velocity structure of the H<sub>2</sub>O masers.

In Table 2, we derived the absolute proper motion of the reference maser spot at the LSR velocity of 20.6 km s<sup>-1</sup>. In addition, we also derived the relative proper motions for other maser spots with respect to this reference spot. As a result, the northern spots at the LSR velocity of 7.1-7.7 km s<sup>-1</sup> are found to be moving away from the reference spot. The average of the proper motions is 10.7 mas yr<sup>-1</sup> or 11.9 km s<sup>-1</sup> with the position angle of -34 degrees ( $\mu_\alpha \cos \delta = -5.9$  mas yr<sup>-1</sup>,  $\mu_\delta = 8.9$  mas yr<sup>-1</sup>) with respect to the reference spot. Based on the fact that the observed red-shifted jet lobe should be expanding toward the southeast direction (Girart &

Acord 2001), the above motion could be naturally interpreted that the southern components are systematically moving toward the southeast direction with respect to the northern one. It is consistent with the expected position of the protostar located at the northwest of the masers as mentioned in the previous section. If this is the case, the maser spots with larger proper motion tends to be distributed away from the driving source.

The radial velocity distribution of the  $\text{H}_2\text{O}$  masers shown in Figure 3 also suggests that the higher velocity components ( $20 \text{ km s}^{-1}$ ) are distributed at the more distant positions from the powering source, which is possibly at the northwest of the masers, than the lower velocity components ( $7 \text{ km s}^{-1}$ ). In addition, the LSR velocities within the southern maser feature gradually increase from  $19 \text{ km s}^{-1}$  at the northern end to  $21 \text{ km s}^{-1}$  at the southern end (Figure 3(c)). Therefore, both the proper motion and radial velocity structure might exhibit an apparent acceleration of the jet driven by the protostar L1448C.

Based on the velocity shift in both the proper motion and the radial velocity between the northern and southern features, we roughly estimate the inclination angle of the maser jet to the line of sight to be 43 degrees. This is smaller than that of the kinematic model proposed for large-scale bipolar outflow, 70 degrees, even if the opening angle of the red-shifted jet lobe, 30 degrees, is taken into account (Bachiller et al. 1995; Girart & Acord 2001). Although our estimation of the inclination angle would contain large uncertainty, this result suggests an evidence for the precession of the jet axis.

As shown in Figure 3, the maser spots are aligned along the northwest-southeast direction. We obtained the position angle of the alignment of the  $\text{H}_2\text{O}$  maser features to be  $-15$  degrees on average. This is in good agreement with that of the large-scale collimated molecular outflow from L1448C,  $-21$  degrees (e.g. Bachiller et al. 1995), while slightly different from the direction of the proper motion as mentioned above,  $-34$  degrees. According to the Spitzer IRAC2 image in Figure 1, the infrared jet is almost parallel to the  $\text{H}_2\text{O}$  masers while it shows slightly curved structure at the northern part of the jet. This is thought to be an evidence for the interaction with the jet and ambient gas around another protostar L1448N (Bachiller et al. 1995). In addition, Hirano et al. (2010) found the deflection of the both blue-shifted and red-shifted  $\text{SiO}$  jet with almost point-symmetry with respect to its driving source, which is possibly caused by the orbital motion of the binary system. Thus, it is likely that the variation in the position angles of the jets derived from the different tracers would be due to the precession of the jet axis. It should be noted that a possible evidence for the precession is also reported for the  $\text{H}_2\text{O}$  maser jet in NGC 1333 IRAS4 (Marvel et al. 2008; Desmurs et al. 2009).

We could evaluate the timescale of the maser jet to be at least 9 years based on the velocity difference in the proper motion between the northern and southern maser features. If the maser spots are accelerated at a constant rate ( $10.7 \text{ mas yr}^{-1}/9 \text{ yr}=1.2 \text{ mas yr}^{-1} \text{ yr}^{-1}$ ), the proper motion would increase by  $0.6 \text{ mas yr}^{-1}$  within the monitoring period of 0.5 year. Although such acceleration might affect the accuracy of the annual parallax and proper motion

measurements, we could not see significant deviation from the linear proper motion with respect to the reference spot within the fitting errors. It would mean that the physical gas clumps appeared as the H<sub>2</sub>O maser features are not really accelerated for 9 years but they just represent the velocity structure of the jet showing apparent acceleration.

The kinematics of the H<sub>2</sub>O maser jet and its time scale are still uncertain mainly because we could not detect the blue-shifted H<sub>2</sub>O maser features. In order to reveal the launching mechanism of the protostellar jet associated with L1448C, which might be the binary system (Hirano et al. 2010), proper motion measurements of both red- and blue-shifted masers would be a key issue.

#### 4.2. Overall structure of the Perseus molecular cloud complex

The present astrometric observations with VERA imply that the distance to L1448C is most likely 232 pc, which is in excellent agreement with that of our previous results for NGC 1333 SVS13A,  $235 \pm 18$  pc (Hirota et al. 2008a). Because the angular separation between these two sources, 1 degree, corresponds to the linear size of 5 pc, the similar extent along the line of sight is also plausible. Although we could not distinguish the difference in their distances, more precise parallax measurements will allow us to reveal the depth of the molecular cloud.

Our distance measurements are consistent with the photometric distance to NGC 1333 reported by Černis (1990) of 220 pc with an uncertainty of 25% rather than the larger value of about 300 pc (e.g. Herbig & Jones 1983; de Zeeuw et al. 1999). Therefore, the present result provides a constraint on the distance to the western part of the Perseus molecular cloud complex to be closer value.

Enoch et al. (2006) suggested that a single distance for the whole of the Perseus molecular cloud complex might not be appropriate although they adopted the distance of 250 pc for the entire area of the Perseus region. According to the photometric observations by Černis (1990) and Černis (1993), there exists a gradient in the distances across the Perseus molecular cloud complex. NGC 1333 is proposed to be the nearest cloud at a distance of 220 pc (Černis 1990) while IC348 is more distant, 300 pc (Černis 1993). The latter value is consistent with that of the Hipparcos result ( $318 \pm 27$  pc; de Zeeuw et al. 1999). Thus, it would be interesting to carry out VLBI astrometry of the H<sub>2</sub>O maser sources and radio emitting T-Tauri stars (e.g. Loinard et al. 2005) in other Perseus clouds, in particular for the eastern part of the complex such as B1, IC348, and B5 (see Figure 5).

As listed in Table 2, the absolute proper motion of the reference maser spot is  $31.8 \text{ mas yr}^{-1}$  or  $35.3 \text{ km s}^{-1}$  toward southeast with the position angle of 137 degrees. The direction of the proper motion seems to be consistent with those of NGC1333 SVS13A (Hirota et al. 2008a) as plotted in Figure 5. It is also reported that the average proper motion for the radio continuum sources in NGC 1333 agrees well with those of the H<sub>2</sub>O masers (Carrasco-González et al. 2008). These systematic motion could be indicative of the proper motion of the Perseus

molecular cloud itself. The larger proper motions for L1448C than NGC1333 SVS13A might be caused by the contamination of the jet motion. High-resolution interferometric observations of continuum emission from YSOs at the centimeter, millimeter, and submillimeter wavelengths with EVLA and ALMA will be crucial to distinguish the contribution from proper motions of outflows, stars, and host clouds.

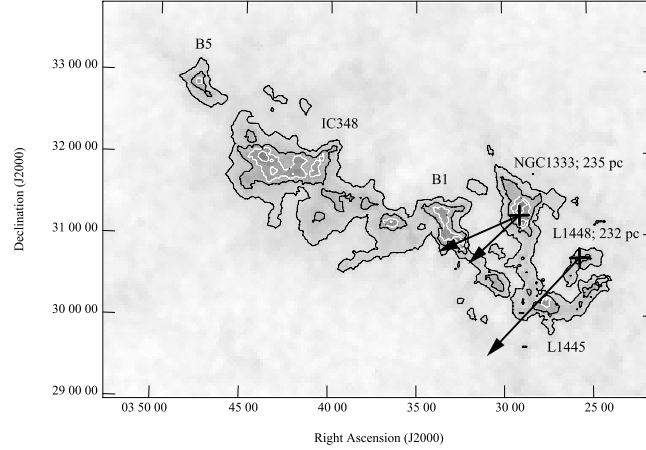


**Fig. 5.** Absolute proper motions of the  $\text{H}_2\text{O}$  masers in L1448C and NGC 1333 SVS13A (Hirota et al. 2008a). Grey scale shows the visual extinction ( $A_V$ ) map derived from the 2MASS data (Ridge et al. 2006). Contour levels are  $A_V=3, 5, 7$ , and 9 magnitude. Crosses and arrows represent the position of the maser sources and their absolute proper motion vectors, respectively.

We are grateful to the staff of all the VERA stations for their assistance in observations. TH is financially supported by Grant-in-Aids from the Ministry of Education, Culture, Sports, Science and Technology (13640242, 16540224, and 20740112).

## References

- Bachiller, R., André, P., Cabrit, S. 1991, *A&A*, 241, L43  
 Bachiller, R., Cernicharo, J., Martín-Pintado, J. Tafalla, M., & Lazareff, B. 1990, *A&A*, 231, 174  
 Bachiller, R., Guilloteau, S., Dutrey, A., Planesas, P., & Martín-Pintado, J. 1995, *A&A*, 299, 857  
 Bally, J., Lada, E. A., & Lane, A. P. 1993, *ApJ*, 418, 322  
 Barsony, M., Ward-Thompson, D., André, P., & O’Linger, J. 1998, *ApJ*, 509, 733  
 Carrasco-González, C., Anglada, G., Rodríguez, L. F., Torrelles, J. M., & Osorio, M. 2008, *AJ*, 136, 2238  
 Černis, K. 1993, *Baltic Astron.*, 2, 214  
 Černis, K. 1990, *Ap&SS*, 166, 315  
 Chernin, L. M. 1995, *ApJ*, 440, L97  
 Chikada, Y., et al. 1991, in *Frontiers of VLBI*, ed. H. Hirabayashi, M. Inoue, & H. Kobayashi (Tokyo: Universal Academy Press), 79

- Claussen, M. J., Wilking, B. A., Benson, P. J., Wootten, A., Myers, P. C., Terebey, S. 1996, *ApJS*, 106, 111
- Curiel, S., Raymond, J. C., Rodríguez, L. F., Cantó, J., & Moran, J. M. 1990, *ApJ*, 365, L85
- Dame, T. M., et al. 1987, *ApJ*, 322, 706
- Desmurs, J.-F., Codella, C., Santiago-García, J., Tafalla, M., Bachiller, R. 2009, *A&A*, 498, 753
- de Zeeuw, P. T., Hoogerwerf, R., de Bruijne, J. H. J., Brown, A. G. A., Blaauw, A. 1999, *AJ*, 117, 354
- Enoch, M. L. et al. 2006, *ApJ*, 638, 293
- Evans, N. J. II, et al. 2003, *PASP*, 115, 965
- Girart, J. M. & Acord, J. M. P. 2001, *ApJ*, 552, L63
- Herbig, G. H., Jones, B. F. 1983, *AJ*, 88, 1040
- Hirano, N., Ho, P. T. P., Liu, S.-Y., Shang, H., Lee, C. -F., Bourke, T. L. 2010, *ApJ*, in press
- Hirota, T. et al. 2007, *PASJ*, 59, 897
- Hirota, T. et al. 2008a, *PASJ*, 60, 37
- Hirota, T. et al. 2008b, *PASJ*, 60, 961
- Honma, M. et al. 2003, *PASJ*, 55, L57
- Honma, M. et al. 2007, *PASJ*, 59, 889
- Honma, M. et al. 2008a, *PASJ*, 60, 935
- Honma, M., Tamura, Y., & Reid, M. J., 2008b, *PASJ*, 60, 951
- Iguchi, S., Kurayama, T., Kawaguchi, N., Kawakami, K. 2005, *PASJ*, 57, 259
- Imai, H. et al. 2007, *PASJ*, 59, 1107
- Jørgensen, J. K. et al. 2006, *ApJ*, 645, 1246
- Kim, M. K. et al. 2008, *PASJ*, 60, 991
- Loinard, L., Mioduszewski, A. J., Rodríguez, L. F., González, R. A., Rodríguez, M. I., Torres, R. M. 2005, *ApJ*, 619, L179
- Loinard, L. Torres, R. M., Mioduszewski, A. J., Rodríguez, L. F., González-Lópezlira, R. A., Lachaume, R., Vázquez, V., & González, E. 2007, *ApJ*, 671, 546
- Loinard, L., Torres, R. M., ; Mioduszewski, A. J., & Rodríguez, L. F. 2008, *ApJ*, 675, L29
- Lynds, B. T. 1962, *ApJS*, 7, 1
- Marvel, K. B., Wilking, B. A., Claussen, M. J., & Wootten, A. 2008, *ApJ*, 685, 285
- Menten, K. M., Reid, M. J., Forbrich, J., & Brunthaler, A. 2007, *A&A*, 474, 515
- Moscadelli, L., Reid, M. J., Menten, K. M., Brunthaler, A., Zheng, X. W., & Xu, Y. 2009, *ApJ*, 693, 406
- Perryman, M. A. C., et al. 1997, *A&A*, 323, L49
- Petrov, L., Kovalev, Y. Y., Fomalont, E. B., & Gordon, D. 2006, *AJ*, 131, 1872
- Petrov, L., Hirota, T., Honma, M., Shibata, K. M., Jike, T., & Kobayashi, H. 2007, *AJ*, 133, 2487
- Reipurth, B., Rodríguez, L. F., Anglada, G., & Bally, J. 2002, *AJ*, 124, 1045
- Ridge, N. et al. 2006, *AJ*, 131, 2921
- Sandstrom, K. M., Peek, J. E. G., Bower, G. C., Bolatto, A. D., & Plambeck, R. L. 2007, *ApJ*, 667, 1161
- Tobin, J. J., Looney, L. W., Mundy, L. G., Kwon, W., & Hamidouche, M. 2007, *ApJ*, 659, 1404

- Torres, R. M., Loinard, L., Mioduszewski, A. J., & Rodríguez, L. F. 2007, *ApJ*, 671, 1813
- Torres, R. M., Loinard, L., Mioduszewski, A. J., & Rodríguez, L. F. 2009, *ApJ*, 698, 242
- Ulich, B. L., Haas, R. W. 1976, *ApJS*, 30, 247